

## Predictions on three-particle azimuthal correlations in proton–proton collisions

Şener ÖZÖNDER<sup>1,2,\*</sup>

<sup>1</sup>Department of Physics, İstanbul Technical University, İstanbul, Turkey

<sup>2</sup>Department of Physics, Koç University, İstanbul, Turkey

Received: 06.10.2017

Accepted/Published Online: 30.11.2017

Final Version: 13.02.2018

**Abstract:** The ridge signal, which is long-ranged in rapidity, in di-hadron correlations in high-multiplicity p–p and p–A collisions opened up a whole new research area in high-energy QCD. Although the ridge had been observed in A–A collisions and interpreted as a result of the radial flow of quark–gluon plasma, it had not appeared until recently in the data of small collision systems such as p–p and p–A, nor had it been predicted theoretically or seen in event generators. There are two competing approaches that attempt to explain the systematics of the di-hadron ridge signal: hydrodynamics and gluon saturation physics (color glass condensate/glasma). In this work, we present predictions for the transverse momentum and rapidity dependence of the three-particle correlation function within gluon saturation physics. Tri-hadron correlations can be measured, and the data can possibly rule out one of the two alternative approaches.

**Key words:** Particle correlations & fluctuations, collective flow, gluon saturation

### 1. Introduction

In the relativistic proton (p) and nucleus (A) collisions, hundreds of hadrons (pions, kaons etc.) and baryons (protons, neutrons etc.) are produced, and the transverse momentum  $p_{\perp}$ , rapidity  $\eta$ , and azimuthal angle  $\phi$  of each particle are measured. The correlations between the particles in rapidity and azimuthal angle at a given transverse momentum interval often reveal interesting information about the particle production mechanism in collisions as well as the evolution of the interacting gas of particles until they freeze out and reach the detectors.

The lowest-order correlation function is the two-particle correlation function  $C_2$ , and it is a function of the azimuthal angle difference  $\Delta\phi = \phi_1 - \phi_2$ , rapidity difference  $\Delta\eta = \eta_1 - \eta_2$ , and the two transverse momenta of gluon pairs. On the theory side, one calculates the two-gluon correlation function, and convolves it with fragmentation functions to obtain hadronic correlation function, which is measured in experiments. One typically investigates whether the particle pairs are correlated when their azimuthal angles are at particular relative values such as  $\phi_1 \sim \phi_2$  and  $\phi_1 \sim \phi_2 + \pi$ , and whether these correlations are preserved even while the rapidity difference  $\Delta\eta$  between the particles extends for several units.

The high-multiplicity ( $N_{\text{trk}}^{\text{offline}} \geq 110$ ) p–p collisions at the LHC at  $\sqrt{s} = 7$  TeV revealed a very interesting phenomenon, which later was also seen in p–Pb collisions. For the first time in p–p collisions, it has been observed that the strength of the correlations between the produced hadrons at  $\phi_1 \sim \phi_2$  was preserved even when hadron pairs were separated for up to four units of rapidity,  $\Delta\eta \sim 4$  [1–4]. These correlations are called the ridge since they appear as a ridge when the di-hadron correlation function is plotted with respect to  $\Delta\eta$  and  $\Delta\phi$ , and they are known to arise from radial expansion of the quark gluon plasma in A–A collisions [5]. However, no such

\*Correspondence: ozonder@uw.edu

fluid flow or creation of quark gluon plasma had been anticipated in p–p or p–Pb collisions. Moreover, Monte Carlo event generators had not predicted the emergence of ridge correlations in these small systems where the target and projectile overlap is small in comparison to that of A–A collisions. The ridge correlations have been observed later in high multiplicity p–Pb collisions as well [4, 6–13].

In this work, we work in the gluon saturation/glasma framework, where no fluid flow or creation of quark gluon plasma is necessary for the emergence of long-range azimuthal ridge correlations [14–22]. Gluon saturation occurs when the density of gluons in a nucleon increases and individual gluons start to overlap. At high energies, the gluon density in the nucleon or nucleus becomes so high that one can think of a nucleon or nucleus as a classical gluon field instead of an individual gluon<sup>1</sup>. It has been shown in Refs. [23–28] that the glasma diagrams featuring gluon saturation gave rise to ridge correlations and they successfully explained the systematics of the data, i.e. the change in the correlation strength with multiplicity,  $p_\perp$ ,  $\Delta\phi$ , and  $\Delta\eta$ .

The scale that gluon saturation becomes important and consequently the classical gluon field approximation for the nucleon or nucleus becomes justified is determined by the saturation scale. The saturation scale increases with increasing beam energy  $\sqrt{s}$ , with which also the multiplicity of produced hadrons increases. That the ridge correlations only appear at high multiplicity events is evidence of the onset of gluon saturation. Furthermore, the ridge correlations are long-ranged in rapidity, and this can be explained in this framework where the running coupling Balitsky–Kovchegov (rcBK) unintegrated gluon distribution (UGD) functions are used to calculate the two-particle correlations. These UGDs feature gluon saturation and they have been calculated by evolving the parton distributions functions in Bjorken- $x$  variable<sup>2</sup>.

Despite the success of the glasma model explaining the systematics of the two-particle ridge signal, the debate as to whether the ridge arises from gluon saturation or a small quark gluon plasma possibly formed in the p–p and p–Pb collisions has not been settled yet. In Refs. [29–31], we suggested that investigating three-hadron correlations could rule out one of the two mechanisms.

In this work, we first show the formula for the three-gluon correlation function  $C_3$ . Then we present our results on the three-particle correlation function calculated with the rcBK wavefunctions. We also make some predictions on the dependence of  $C_3$  on  $p_\perp$  and  $y_p$  ( $=\eta_p$ ) in p–p collisions at  $\sqrt{s} = 7$  TeV. These results can be compared with the data when  $C_3$  is measured in the future.

## 2. Three-particle azimuthal correlation function

The triple-gluon inclusive distribution function is given by [29]

$$C_3 = \frac{\alpha_s^3 N_c^3 S_\perp}{\pi^{12} (N_c^2 - 1)^5} \frac{1}{\mathbf{p}_\perp^2 \mathbf{q}_\perp^2 \mathbf{l}_\perp^2} \int \frac{d^2 \mathbf{k}_\perp}{(2\pi)^2} (\mathcal{T}_1 + \mathcal{T}_2), \quad (1)$$

where

$$\mathcal{T}_1 = 2 \times (\Phi_{1,p}(\mathbf{k}_\perp))^2 \Phi_{1,q}(\mathbf{k}_\perp) \Phi_{2,p}(\mathbf{p}_\perp - \mathbf{k}_\perp) \mathcal{T}_{A_2}, \quad (2)$$

$$\mathcal{T}_2 = 2 \times (\Phi_{2,i}(\mathbf{k}_\perp))^2 \Phi_{2,q}(\mathbf{k}_\perp) \Phi_{1,p}(\mathbf{p}_\perp - \mathbf{k}_\perp) \mathcal{T}_{A_1}, \quad (3)$$

and

<sup>1</sup>The density of quarks in the wavefunction of a nucleon or nucleus is vanishingly small with respect to the density of gluons at high energies. This can be seen through parton distribution functions of quarks and gluons.

<sup>2</sup>This is in contrast to the DGLAP evolution where the parton distribution functions are evolved in  $Q^2$ .

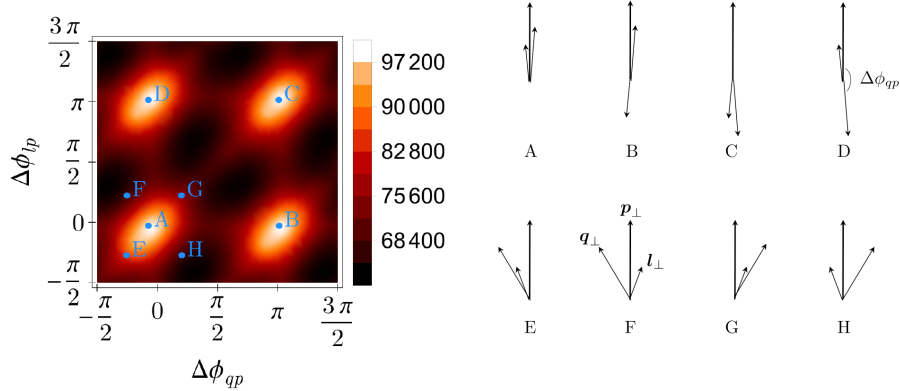


**Figure 1.** (left) The density plot of  $C_3(\Delta\phi_{qp}, \Delta\phi_{lp})$  in arbitrary units at transverse momenta  $p_\perp = q_\perp = l_\perp = 2 \text{ GeV}$  and rapidities  $y_p = y_q = y_l = 0$ . (right) Here  $p_\perp$  is chosen as the trigger particle and so its azimuthal position is fixed. The two azimuthal angle differences ( $\Delta\phi_{qp}$  and  $\Delta\phi_{lp}$ ) are measured from the azimuthal position of gluon with momentum  $p_\perp$ . This figure shows some possible azimuthal configurations of the three gluons as marked with letters on the density plot [29].

$$\mathcal{T}_{A_1(A_2)} = [\Phi_{1(2),q}(\mathbf{q}_\perp - \mathbf{k}_\perp) + \Phi_{1(2),q}(\mathbf{q}_\perp + \mathbf{k}_\perp)] \quad (4)$$

$$\times [\Phi_{1(2),l}(\mathbf{l}_\perp - \mathbf{k}_\perp) + \Phi_{1(2),l}(\mathbf{l}_\perp + \mathbf{k}_\perp)]. \quad (5)$$

Here  $\alpha_s$  is the strong coupling constant,  $N_c = 3$  is number of colors in QCD, and  $S_\perp$  is the overlap area of the target and projectile. The first index of the UGD  $\Phi$  is 1 or 2, and it refers to the projectile and target. The second index of the UGD is the rapidity variable of the produced gluon, and  $\mathbf{p}_\perp$ ,  $\mathbf{q}_\perp$ , and  $\mathbf{l}_\perp$  are the transverse momenta variables of the gluons produced.

To calculate the three-gluon correlation function, we use rcBK UGDs [14, 32–35]. The details of evolution of these proton wavefunctions with rapidity are given in Ref. [29].

For three gluons, there are two azimuthal angle differences ( $\Delta\phi_{qp} = \phi_q - \phi_p$  and  $\Delta\phi_{lp} = \phi_l - \phi_p$ ) and two rapidity differences ( $\Delta\eta_{qp} = \eta_q - \eta_p$  and  $\Delta\eta_{lp} = \eta_l - \eta_p$ ). Also considering the magnitude of the transverse momenta of the three gluons, the correlation function can be expressed as

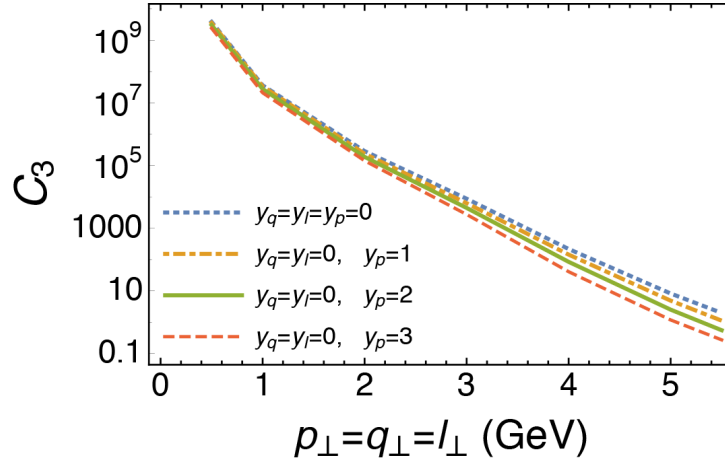
$$C_3 \equiv C_3(\Delta\phi_{qp}, \Delta\phi_{lp}, \Delta\eta_{qp}, \Delta\eta_{lp}, p_\perp, q_\perp, l_\perp). \quad (6)$$

Figure 1 shows a density plot of  $C_3$  along with several azimuthal configurations that different points on the plot correspond to.

### 3. Systematics of three-gluon correlations

In this section, we shall explore how  $C_3$  changes with transverse momentum and rapidity of the three gluons. In Ref. [29], we showed that  $C_3$  became maximum when  $\{\Delta\phi_{qp}, \Delta\phi_{lp}\} \approx \{\{0, 0\}, \{0, \pi\}, \{\pi, 0\}, \{\pi, \pi\}\}$ . This is in line with the finding that the peak in the two-particle ridge correlations  $C_2$  occurred at  $\Delta\phi_{qp} \approx 0$  and  $\Delta\phi_{lp} \approx \pi$  [14–22]. To study the momentum and rapidity dependence of  $C_3$ , here we shall calculate it at one of its peak values with respect to the two azimuthal angle differences; we arbitrarily choose this point to be  $\{\Delta\phi_{qp}, \Delta\phi_{lp}\} = \{0, 0\}$ . This point corresponds to the position marked as “A” in Figure 1.

One of the hallmarks of the two-particle ridge correlations data is that the magnitude of the peak at  $\Delta\phi_{qp} \approx 0$  is preserved even if the two particles are separated by several units of rapidity [14–22]. In the framework of saturation physics, this is attributed to the gluon saturation and relatively slow evolution of the nucleon wavefunctions with small- $x$  in the Bjorken limit of QCD. On the other hand, studies show that application of hydrodynamics to p–p and p–Pb collisions could also produce ridge correlations—without resorting to gluon saturation—due to the assumed hydrodynamization and consequent radial flow [36–41]. In order to better understand the actual mechanism behind how the long-ranged rapidity correlations arise, examining the three-particle correlations both in the saturation physics and hydrodynamics frameworks is in order. Below, we show the dependence of  $C_3$  on transverse momentum and rapidity of one of the three gluons.



**Figure 2.** Log-linear plot of the three-gluon correlation function  $C_3$  vs. the transverse momenta of the gluons  $p_\perp = q_\perp = l_\perp$  for p–p collisions at  $\sqrt{s} = 7$  TeV.  $C_3$  in the graph is in units of  $\alpha_s^3 N_c^3 S_\perp / [\pi^{12} (N_c^2 - 1)^5]$ . Different curves correspond to different rapidity values of the gluon with the rapidity  $y_p$ .

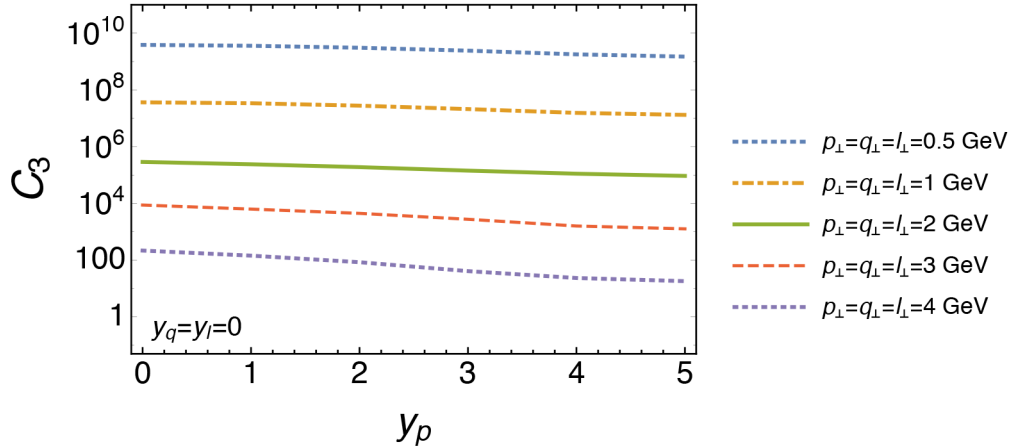


**Figure 3.** Log-linear plot of the three-gluon correlation function  $C_3$  vs. the rapidity  $y_p$  for p–p collisions at  $\sqrt{s} = 7$  TeV. Here  $y_q$  and  $y_l$  are taken to be zero.  $C_3$  in the graph is in units of  $\alpha_s^3 N_c^3 S_\perp / [\pi^{12} (N_c^2 - 1)^5]$ .

The results of this work are shown in Figures 2 and 3. That the three-gluon correlations are large at low- $p_\perp$  has also been observed in the two-particle correlation calculations and measurements; this is understood

as a manifestation of the semihard gluon saturation scale,  $Q_s \sim 1$  GeV [23–28]. As for the rapidity dependence of  $C_3$ , we observe that the correlation strength decreases approximately as power-law with increasing rapidity gap between the gluons. This is in contrast to the two-particle correlations where the correlation strength is approximately constant with increasing rapidity difference.

#### 4. Summary and Outlook

We presented results on the transverse momentum and rapidity dependence of the three-gluon correlation function in the gluon saturation/glasma framework. Our preliminary predictions are based on the gluonic correlation function  $C_3$ , and in order to obtain the hadronic correlation function, our results need to be convolved with the fragmentation function; this is a subject for further work. However, we expect that the essential features of our results based on the gluonic correlation function would be preserved in the hadronic correlation function. The three-hadron correlations in p–p collisions at  $\sqrt{s} = 7$  GeV have not been measured yet. Our results can be compared with the data when  $C_3$  is measured in the future. We expect our work to be the next step—after the study of di-hadron correlations—towards understanding the true origins of the correlations in p–p and p–A collisions.

#### Acknowledgment

This work was funded by the Scientific and Technological Research Council of Turkey (TÜBİTAK) BİDEB 2232-117C008.

#### References

- [1] Khachatryan, V.; Sirunyan A.M.; Tumasyan A.; Adam, W.; Bergauer, T.; Dragicevic, M.; Er, J.; Fabjan, C.; Friedl, M.; Fruehwirth, R.; et al. *J. High Energy Phys.* **2010**, 1009, 091.
- [2] Velicanu, D. *J. Phys. G* **2011**, 38, 124051.
- [3] Li, W. *Mod. Phys. Lett. A* **2012**, 27, 1230018.
- [4] Wozniak, K. W. *J. Phys. Conf. Ser.* **2017**, 779, 012057.
- [5] Dumitru, A.; Gelis, F.; McLerran, L.; Venugopalan, R. *Nucl. Phys. A* **2008**, 810, 91-108.
- [6] Chatrchyan, S.; Khachatryan, V.; Sirunyan A.M.; Tumasyan A.; Adam, W.; Aguilo, R., Bergauer, T.; Dragicevic, M.; Er, J.; Fabjan, C.; et al. *Phys. Lett. B* **2013**, 718, 795-814.
- [7] Avelev, B. B.; Adam, J.; Adamova, D.; Adare, A. M.; Aggarwal, M.; Rinella, G. A.; Agnello, M.; Agocs, A. G.; Agostinelli, A.; Ahammed, Z. et al., *Phys. Lett. B* **2013**, 719, 29-41.
- [8] Aad, G.; Abajyan, T.; Abbott, B.; Abdallah, J.; Khalek, S. A.; Abdelalim, A. A.; Abdinov, O.; Aben, R.; Abi, B.; Abolins, M. et al., *Phys. Rev. Lett.* **2013**, 110, 182302.
- [9] Milano, L. *Nucl. Phys. A* **2014**, 931, 1017-1021.
- [10] Avelev, B. B.; Adam, J.; Adamova, D.; Adare, A. M.; Aggarwal, M.; Rinella, G. A.; Agnello, M.; Agocs, A. G.; Agostinelli, A.; Ahammed, Z.; et al. *Phys. Lett. B* **2013**, 726, 164-177.
- [11] Avelev, B. B.; Adam, J.; Adamova, D.; Adare, A. M.; Aggarwal, M.; Rinella, G. A.; Agnello, M.; Agostinelli, A.; Agrawal, N.; Ahammed, Z.; et al. *Phys. Rev. C* **2014**, 90, 054901.
- [12] Avelev, B. B.; Adam, J.; Adamova, D.; Aggarwal, M.; Agnello, M.; Rinella, G. A.; Agnello, M.; Agostinelli, A.; Agrawal, N.; Ahammed, Z.; et al. *Phys. Lett. B* **2015**, 741, 38-50.
- [13] Aad, G.; Abbott, B.; Abdallah, J.; Khalek, S. A.; Abdinov, O.; Aben, R.; Abi, B.; Abolins, M.; AbouZeid, O.; Abramowicz, H.; et al. *Phys. Rev. C* **2014**, 90, 044906.

- [14] Dusling, K.; Gelis, F.; Lappi, T.; Venugopalan, R. *Nucl. Phys. A* **2010**, *836*, 159-182.
- [15] Dusling, K.; Fernandez-Fraile, D.; Venugopalan, R. *Nucl. Phys. A* **2009**, *828*, 161-177.
- [16] Kovner, A.; McLerran, L. D.; Weigert, H. *Phys. Rev. D* **1995**, *52*, 3809-3814.
- [17] Kovchegov, Y. V.; Rischke, D. H. *Phys. Rev. C* **1997**, *56*, 1084-1094.
- [18] Gelis, F.; Lappi, T.; McLerran, L. *Nucl. Phys. A* **2009**, *828*, 149-160.
- [19] McLerran, L. D.; Venugopalan, R. *Phys. Rev. D* **1994**, *49*, 2233-2241.
- [20] McLerran, L. D.; Venugopalan, R. *Phys. Rev. D* **1994**, *49*, 3352-3355.
- [21] McLerran, L. D.; Venugopalan, R. *Phys. Rev. D* **1994**, *50*, 2225-2233.
- [22] Kovchegov, Y. V. *Phys. Rev. D* **1996**, *54*, 5463-5469.
- [23] Dumitru, A.; Dusling, K.; Gelis, F.; Jalilian-Marian, J.; Lappi, T.; Venugopalan, R. *Phys. Lett. B* **2011**, *697*, 21-25.
- [24] Dusling, K.; Venugopalan, R. *Phys. Rev. Lett.* **2012**, *108*, 262001.
- [25] Dusling, K.; Venugopalan, R. *Phys. Rev. D* **2013**, *87*, 051502.
- [26] Dusling, K.; Venugopalan, R. *Phys. Rev. D* **2013**, *87*, 054014.
- [27] Dusling, K.; Venugopalan, R. *Phys. Rev. D* **2013**, *87*, 094034.
- [28] Venugopalan, R. *Annals Phys.* **2015**, *352*, 108-116.
- [29] znder, . *Phys. Rev. D* **2015**, *91*, 034005.
- [30] znder, . *Phys. Rev. D* **2016**, *93*, 054036.
- [31] znder, . *Phys. Rev. D* **2017**, *96*, 074005.
- [32] Balitsky, I. *Nucl. Phys. B* **1996**, *463*, 99-160.
- [33] Kovchegov, Y. V. *Phys. Rev. D* **1999**, *60*, 034008.
- [34] Gelis, F.; Stasto, A. M.; Venugopalan, R. *Eur. Phys. J.* **2006**, *48*, 489-500.
- [35] Fujii, H.; Gelis, F.; Venugopalan, R. *Nucl. Phys. A* **2006**, *780*, 146-174.
- [36] Bozek, P. *Phys. Rev. C* **2012**, *85*, 014911.
- [37] Bozek, P.; Broniowski, W. *Phys. Lett. B* **2013**, *718*, 1557-1561.
- [38] Bozek, P.; Broniowski, W.; Torrieri, G. *Phys. Rev. Lett.* **2013**, *111*, 172303.
- [39] Werner, K.; Bleicher, M.; Guiot, B.; Karpenko, Iu.; Pierog, T. *Phys. Rev. Lett.* **2014**, *112*, 232301.
- [40] Kozlov, I; Luzum, M.; Denicol, G.; Jeon, S.; Gale, C. *arXiv:1405.3976* **2014**.
- [41] Bzdak, A.; Ma, G. L. *Phys. Rev. Lett.* **2014**, *113*, 252301.